Synthesis, Characterization, Crystal structure and Hirshfeld surface analysis of alkyl Substituted N,4-diphenyl thiazole-2-amine.

AfraQuasar A Nadaf , Umashri Kendur , Shivaraj Mantur , Mahesh S. Najare , Manjunatha Garbhagudi , Supreet Gaonkar , Imtiyaz Ahmed M. Khazi

PII: S2405-8300(19)30323-4
DOI: https://doi.org/10.1016/j.cdc.2019.100297
Reference: CDC 100297

To appear in: *Chemical Data Collections*

Received date: 20 August 2019
Revised date: 14 October 2019
Accepted date: 14 October 2019

Please cite this article as: AfraQuasar A Nadaf , Umashri Kendur , Shivaraj Mantur , Mahesh S. Najare , Manjunatha Garbhagudi , Supreet Gaonkar , Imtiyaz Ahmed M. Khazi , Synthesis, Characterization, Crystal structure and Hirshfeld surface analysis of alkyl Substituted N,4-diphenyl thiazole-2-amine., *Chemical Data Collections* (2019), doi: https://doi.org/10.1016/j.cdc.2019.100297

Synthesis, Characterization, Crystal structure and Hirshfeld surface analysis of alkyl Substituted N,4-diphenyl thiazole-2-amine.

AfraQuasar A Nadaf[a], Umashri Kendur[a], Shivaraj Mantur[a], Mahesh S. Najare[a], Manjunatha Garbhagudi [a], Supreet Gaonkar[a] and Imtiyaz Ahmed M. Khazi [a]*

[a]*Department of Chemistry, Karnatak University, Dharwad 580003, Karnataka, India*
Corresponding author mail: drimkorgchem@gmail.com

Abstract

The present work describes the synthesis of 4-(4-bromophenyl)-*N*-(4-chlorophenyl)-*N*-propylthiazol-2-amine (**3a**) and *N*-(4-chlorophenyl)-*N*-ethyl-4-(4-nitrophenyl)thiazol-2-amine (**3b**) through a three step pathway. The synthesized compounds were characterized by ^{1}H NMR, ^{13}C NMR, FT-IR and mass spectral analysis. Further, the structures were confirmed by single crystal X-ray diffraction studies which revealed that **3a** crystallizes in triclinic system with *P*-1 space group whereas **3b** crystallizes as monoclinic with $P2_1/c$ space group. The asymmetric unit consists of only one molecule in both the structures. The study of torsional angles of **3a** and **3b** indicated that S1 and C4 are *cis* to each other whereas N2 and C4 are *trans*. A detailed analysis of intermolecular hydrogen bonding interactions has been performed. Also their C-H···π and π···π stacking interactions have been explored using Hirshfeld surface analysis and their 2D fingerprint plots. The most significant contributions in both the compounds are due to H···H interactions which also account for their stability.

Keywords: 4-(4-bromophenyl)-N-(4-chlorophenyl)-N-propylthiazol-2-amine; N-(4-chlorophenyl)-N-ethyl-4-(4-nitrophenyl)thiazol-2-amine; Hirshfeld surface analysis; Crystal Structure; Single Crystal X-ray diffraction; π···π stacking interactions.

Graphical Abstract

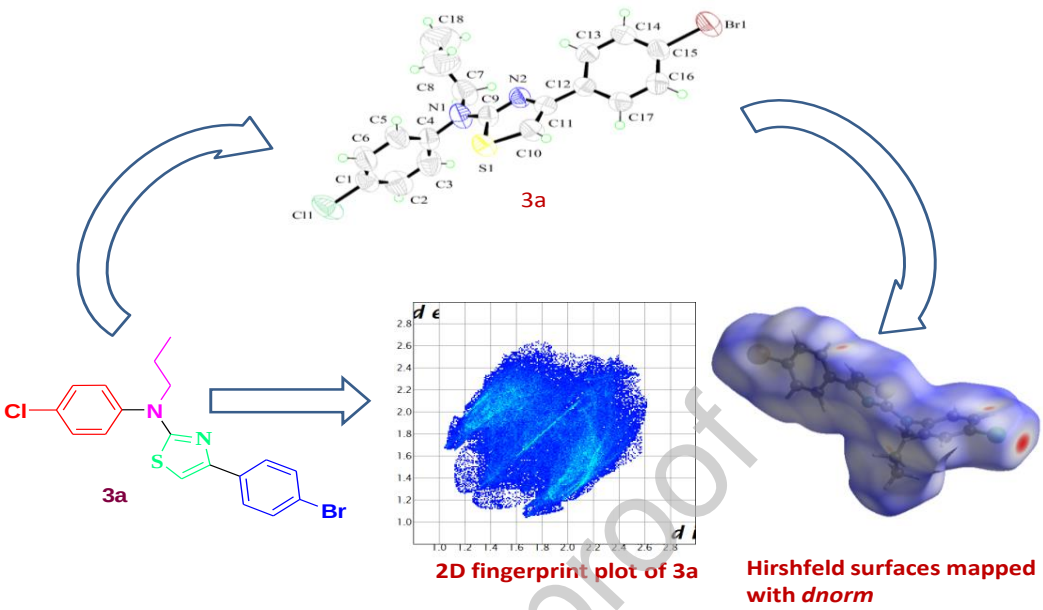

Specifications

Subject area	Organic Chemistry, Spectroscopy, Crystallography.
Compounds	4-(4-bromophenyl)-N-(4-chlorophenyl)-N-propylthiazol-2-amine (3a), N-(4-chlorophenyl)-N-ethyl-4-(4-nitrophenyl)thiazol-2-amine (3b)
Data category	Synthesis, X- ray crystallography.
Data acquisition format	Spectral, Crystallographic Information File (cif).
Data type	Analyzed
Procedure	Compounds 3a and 3b were synthesized, characterized by spectral and SC-XRD study. Data collected and structure was solved. Hirshfeld surface analysis was used to study the interaction in the crystal.
Data accessibility	Crystallographic data reported for the structures in this paper can be obtained from Cambridge Crystallographic Data Centre as Supplementary publication no. CCDC-**1945656** and **1945504**.

Rationale

In the discovery of new drugs, the chemistry of heterocyclic compounds plays a prominent role; the study of their theoretical and practical aspects is also gaining significance [1]. This has encouraged researchers to aim for the synthesis of heterocyclic functional molecules with cheaper raw materials and efficient simple synthetic strategies having wide applications [2]. Amongst the heterocyclic compounds the ones with nitrogen and sulphur atoms in their scaffold are in the forefront of interest due to their remarkable pharmacological properties [3-6]. Thiazole being one such nucleus bearing both these atoms in its framework, along with diverse modifications occupies a unique position in chemistry [7-8]. Although the earlier work on this core moiety began in 1879 by Hoffman, however the systematic study was reported in 1887 from Hantzsch laboratory and then onwards enormous work has been done on it in terms of its synthesis and applications [9-13].

Literature reports a variety of methods for synthesis of 1,3-thiazoles but the most reliable route is the Hantzsch pathway which involves condensation of α-halocarbonyl compounds with thiourea which is efficient as well as eco-compatible [14]. C-N and C-S bonds are the features responsible for thiazole moiety to account for its potential biological activity [15-17]. Substituted thiazoles exhibit a wide range of biological activities and are vital components in most of the commercial drugs such as antineoplastic (Tiazofurin and dasatinib) [18-19], anti-HIV (ritonavir) [20-21], antifungal (ravuconazole) [22], antiparasitic (nitazoxanide) [23-24], anti-inflammatory (fanetizole, meloxicam and fentiazac) [25], antiulcer (nizatidine) and as an insecticide (thiamethoxam) [26]. In addition, trisubstituted and disubstituted 1,3- thiazoles associated to aryl or heteroaryl groups are privileged structural motifs and also find applications in materials science for the preparation of liquid crystals [27], molecular switches [28], sensors [29] and also in cosmetic industry (sunscreens) [30].

To gain insight into the behavior of molecular materials, it is vital to understand their intermolecular interactions which govern the crystal packing of any solid [31]. In this regard we report the synthesis and characterization of 4-(4-bromophenyl)-*N*-(4-chlorophenyl)-*N*-propylthiazol-2-amine (**3a**) and *N*-(4-chlorophenyl)-*N*-ethyl-4-(4-nitrophenyl)thiazol-2-amine (**3b**) by using spectral and SC-XRD studies. In order to quantify the interactions within the crystal structure Hirshfeld surface analysis was employed wherein close intermolecular contacts between the molecules were investigated.

Procedure

Materials and Methods

All the required chemicals and solvents were of reagent grade purchased from Sigma Aldrich and used without further purification. The Melting points were determined and recorded by open capillary method and are uncorrected. The FT-IR spectra were recorded on Perkin Elmer FT-IR spectrometer. ^{1}H and ^{13}C NMR data were collected by using JEOL 400-MHz FT NMR spectrometer in $CDCl_3$. Chemical shifts (δ) are written in parts per million using tetra methyl silane (TMS) as internal standard. Mass spectra were recorded by using GCMS-QP2010S SHIMADZU instrument.

Synthesis of the target compounds

Synthesis of the target compounds is schematically represented in **Scheme 1**. The 3 step process uses eco-friendly conditions and proceeds in a clean pathway. The parent molecule for the target compounds **3a** & **3b** were synthesized as per the reported procedures [32-33].

Synthesis of 1-(4-chlorophenyl) thiourea [1]

p-chloro aniline (1g, 0.0107mmol) and potassium thiocyante (4.17g, 0.043mmol) were taken in a round bottom flask containing conc. HCl (10ml). The mixture was refluxed for overnight at 80 ^{o}C and the completion of the reaction was monitored by TLC. The solid formed in the reaction mixture was filtered and dried. The crude compound was recrystallised using ethanol to obtain the required 1-(4-chlorophenyl) thiourea in pure solid form with 85% yield (1.243g) [32].

Synthesis of 4-(4-bromophenyl)-N-(4-chlorophenyl)thiazol-2-amine [2a] & N-(4-chlorophenyl)-4-(4-nitrophenyl)thiazol-2-amine [2b]

A mixture of equimolar quantities of 1-(4-chlorophenyl) thiourea (1g, 0.0059mmol) synthesized earlier and substituted phenacyl bromides (1.17g 0.0059mmol)[for **2a**: 2-bromo-1-(4-bromophenyl)ethanone, **2b**: 2-bromo-1-(4-nitrophenyl)ethanone)] were taken in ethanol (10ml). The reaction mixture was stirred for 2-5 minutes and progress of the reaction was monitored by TLC. After the completion of reaction, the formed solid was filtered, washed with cold ethanol and dried. The crude compound was recrystallized from ethanol to get substituted N,4-diphenylthiazol-2-amine in pure form as solid with good yields, [for 2a yield 93% (1.38g), 2b yield 89% (1.1g)] [33].

Synthesis of 4-(4-bromophenyl)-N-(4-chlorophenyl)-N-propylthiazol-2-amine [3a] & N-(4-chlorophenyl)-N-ethyl-4-(4-nitrophenyl)thiazol-2-amine [3b]

An equimolar mixture of substituted N,4-diphenylthiazol-2-amine **(2a & 2b)** (400mg, 1.42mmol) and alkyl halide (0.1mL, 1.42mmol) were taken in DMF(10mL) and stirred overnight at r.t in the presence of K_2CO_3. Reaction was monitored by TLC and after the completion of the reaction; it was quenched in ice cold water. The formed solid was filtered, dried and recrystallised using ethanol to get corresponding alkylated product as yellow solid.

Characterization of *4-(4-bromophenyl)-N-(4-chlorophenyl)-N-propylthiazol-2-amine* (3a)

Yellow solid; Yield: 82% (365mg); MP: 90-92 ^{o}C; FT-IR (cm^{-1}): 1376, 1530, 1512; ^{1}H NMR (400 MHz, $CDCl_3$) (δ ppm): 7.70 (d, *J*=8.6 Hz, 2H), 7.49 (d, *J*=8.6 Hz, 2H), 7.41 (d, *J*=8.8 Hz, 2H), 7.32 (d, *J*=8.8 Hz, 2H), 6.64 (s, 1H), 4.01 (t, *J*=7.1 Hz, 2H), 1.73 (m, 2H), 0.97 (t, *J*=7.4 Hz, 3H,); ^{13}C NMR (100 MHz, $CDCl_3$) (δppm): 168.46, 157.71, 132.93, 132.32, 132.04, 127.64, 127.48, 123.47, 115.17, 114.76, 100.18, 55.72, 31.08, 21.19. GC-MS: m/z calcd for $C_{18}H_{16}BrClN_2S$ 407.76, found 408(M^+).

Characterization of *N-(4-chlorophenyl)-N-ethyl-4-(4-nitrophenyl)thiazol-2-amine* (3b)

Yellow solid; Yield: 88% (355mg); MP: 122-124 ^{o}C; FT-IR (cm^{-1}): 1280, 1592, 1530, 1337, 1505, 711; ^{1}H NMR (400 MHz, $CDCl_3$) (δ ppm): 8.23 (d, *J*=8.9 Hz, 2H), 7.98 (d, *J*=8.9 Hz, 2H), 7.43 (d, *J*=8.7 Hz, 2H), 7.34 (d, *J*=8.7 Hz, 2H), 6.89 (s, 1H), 4.08 (q, *J*=7.1 Hz, 2H), 1.32 (t, *J*=7.1 Hz, 3H); ^{13}C NMR (100 MHz, $CDCl_3$) (δ ppm): 169.56, 149.34, 146.81, 143.01, 140.98, 132.98, 130.34, 128.29, 126.48, 124.17, 105.48, 48.33, 13.19; GC-MS: m/z calcd for $C_{17}H_{14}ClN_3O_2S$ 359.83, found 359 (M^+).

Crystallography Data Collection

Defect free single crystals of 4-(4-bromophenyl)-N-(4-chlorophenyl)-N-propylthiazol-2-amine (**3a**) and N-(4-chlorophenyl)-N-ethyl-4-(4-nitrophenyl)thiazol-2-amine (**3b**) were chosen for X-ray Diffraction studies. The X-ray diffraction data of both **3a** and **3b** were collected at 296 K on a Bruker SMART APEX2 CCD area-detector diffractometer using a graphite monochromater MoKα (λ = 0.71073) radiation source. The frames were integrated with the Bruker SAINT Software package using a narrow-frame algorithm. In the absence of anomalous scattering, Friedel pairs were merged. The H atoms were all located in a difference map, but those attached to carbon atoms were repositioned geometrically. The H atoms were initially refined with soft restraints on the bond lengths and angles to regularize their geometry, after which the positions were refined with riding constraints [34]. All non-hydrogen atoms were refined anisotropically.

Structure solution and refinement were performed using Crystals [35]. Molecular graphics were generated using Cameron [36]; structure figures were generated with ORTEP-III [37]. The structures were solved by direct methods and refined against F^2 by full-matrix least-squares using the program SHELXL-2014/6 [38]. Details of the crystallographic data and structure refinement are as given in **Table 1.**

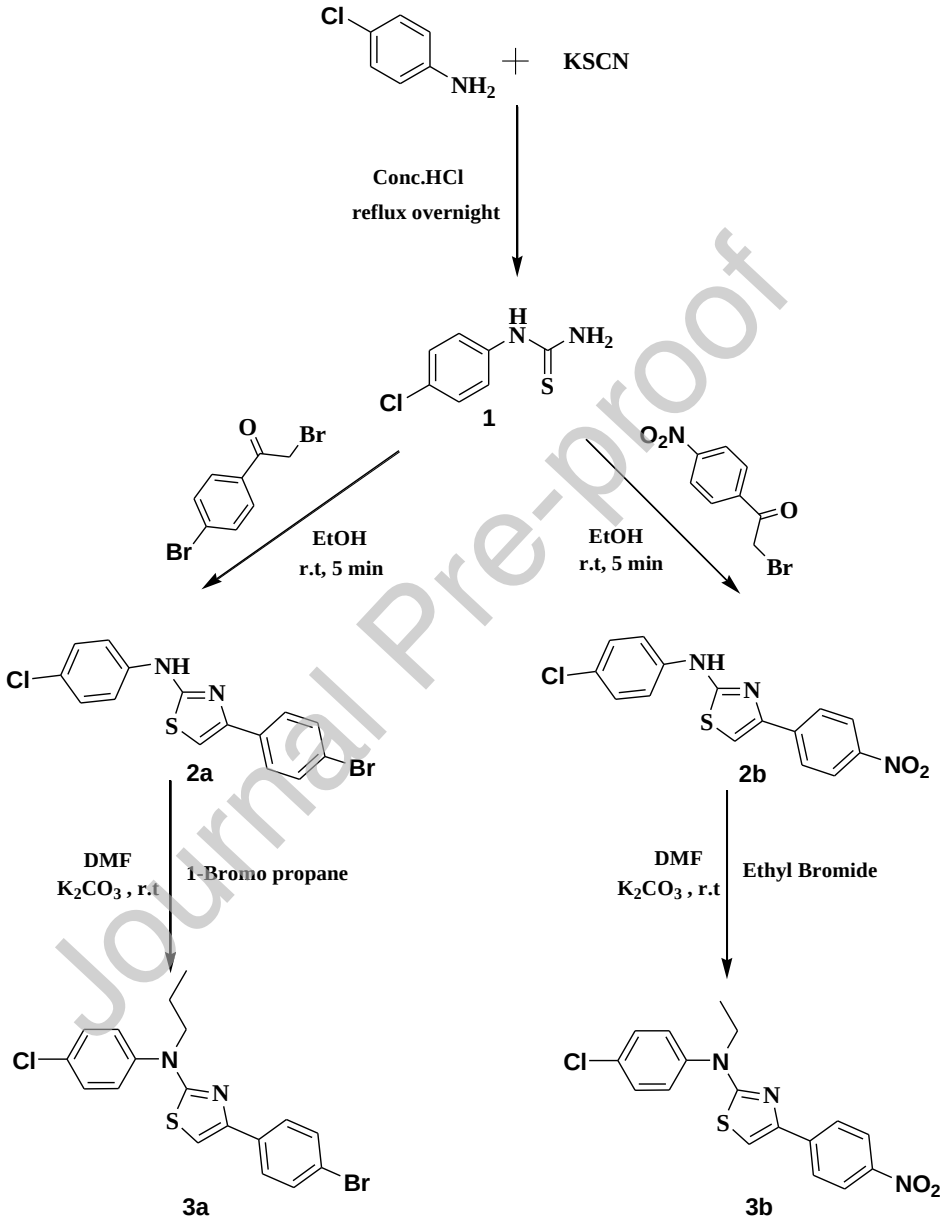

Scheme 1: Synthetic route for the target compounds **3a** & **3b**

Hirshfeld surface analysis

Hirshfeld surfaces (HSs) and 2D fingerprint plots (FPs) were generated using Crystal Explorer 3.1[39] based on results of SC-XRD studies. The function d_{norm} is a ratio encompassing the distances of any surface point to the nearest interior (d_i) and exterior (d_e) atom and the van der Waals radii of the atoms [40]. The negative value of d_{norm} indicates the sum of d_i and d_e is shorter than the sum of the relevant van der Waals radii, which is considered to be the closest contact and is visualized as red color in the HSs. The white color denotes intermolecular distances close to van der Waals contacts with d_{norm} equal to zero whereas contacts longer than the sum of van der Waals radii with positive d_{norm} values are colored with blue. A plot of d_i versus d_e is a 2D fingerprint plot which recognizes the existence of different types of intermolecular interactions.

Table 1. Crystal data and structure refinement details of **3a** and **3b**

Identification code	**3a**	**3b**
Empirical formula	$C_{18}H_{16}BrClN_2S$	$C_{17}H_{14}ClN_3O_2S$
Formula weight	407.75	359.82
Temperature/K	296(2)	296(2)
Crystal system	triclinic	monoclinic
Space group	*P*-1	*P21/c*
a/Å	5.676(2)	10.53(3)
b/Å	10.59(4)	18.72(5)
c/Å	16.13(5)	8.848(2)
α/°	75.27(2)	90
β/°	81.304(2)	103.8(10)
γ/°	76.360(2)	90
Volume/Å^3	906.95(6)	1693.90(8)
Z	2	4
ρ_{calc}g/cm^3	1.493	1.411
μ/mm^{-1}	2.529	0.363
F(000)	412.0	744.0
Radiation	MoKα (λ = 0.71073)	MoKα (λ = 0.71073)
2Θ range for data collection/°	2.624 to 51.888	3.984 to 69.18
Index ranges	$-6 \le h \le 6$, $-12 \le k \le 13$, $-19 \le l \le 19$	$-14 \le h \le 16$, $-25 \le k \le 29$, $-14 \le l \le 14$
Reflections collected	12883	27733
Independent reflections	3475 [R_{int}= 0.0419, R_{sigma}= 0.0458]	7200 [R_{int}= 0.0301, R_{sigma}= 0.0289]
Data/restraints/parameters	3475/0/209	7200/0/217
Goodness-of-fit on F^2	1.008	1.027

Final *R* indexes [*I*>=2σ (*I*)]	R_1= 0.0433, wR_2= 0.1041	R_1 = 0.0571, wR_2= 0.1469
Final *R* indexes [all data]	R_1= 0.0807, wR_2= 0.1231	R_1 = 0.1043, wR_2= 0.1731
Largest diff. peak/hole / e Å^{-3}	0.35/-0.24	0.28/-0.43

Data, value and validation

The compounds **3a** and **3b** crystallized under a triclinic and monoclinic system with space group *P-1* and *P21/c* respectively. The unit cell dimensions of compound **3a** are as follows: a=5.676(2)Å, b=10.59(4)Å, c=16.13(5)Å, α=75.27(2)°, β=81.304(2)°, γ=76.360(2)°, Z= 2. For compound **3b** the unit cell dimensions are: a= 10.53(3) Å, b= 18.72(5) Å, c= 8.848(2) Å, α= 90°, β= 103.8(10)°, γ= 90°, Z= 4. In both the structures the asymmetric unit consists of only one molecule. ORTEP representations of the same showing 50 % displacement ellipsoids along with the numbering scheme are displayed in **Fig.1-2**. Molecular packing and molecular planes are presented in the **Fig.3-6** respectively. Selected bond angles, bond lengths and hydrogen bonding interactions are compiled in **Tables 2-4**, respectively.

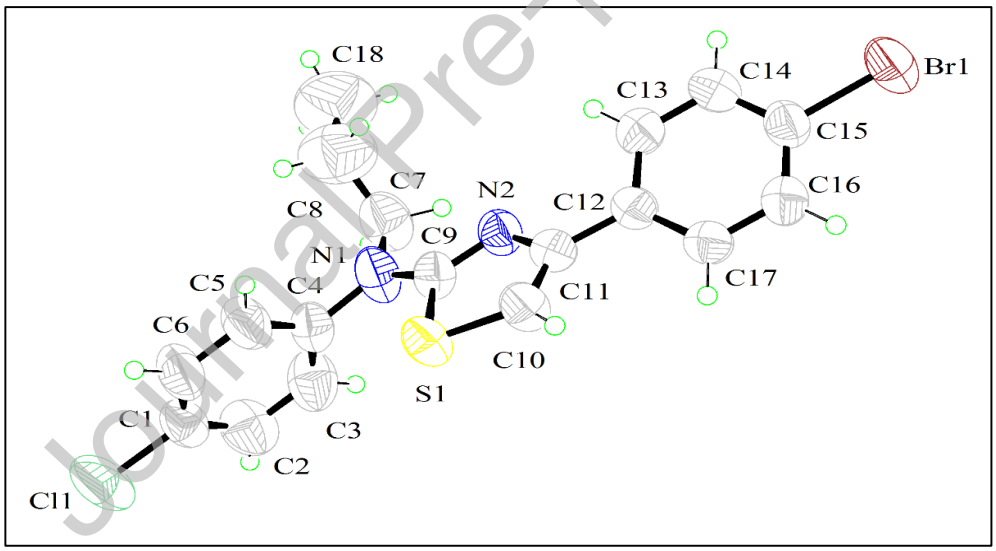

Fig.1. ORTEP diagram of **3a** with thermal ellipsoids drawn at 50% probability

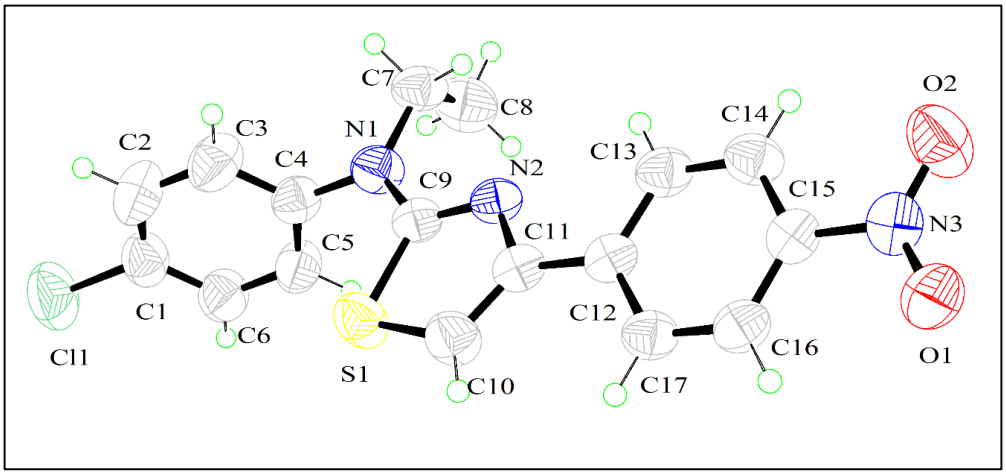

Fig.2. ORTEP diagram of **3b** with thermal ellipsoids drawn at 50% probability

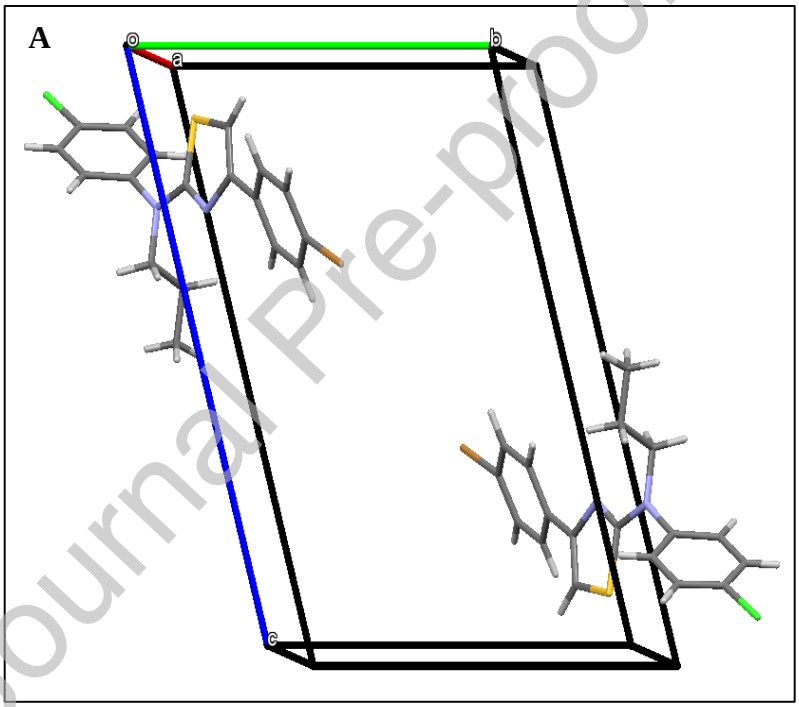

Fig.3. (A) Molecular packing of **3a**

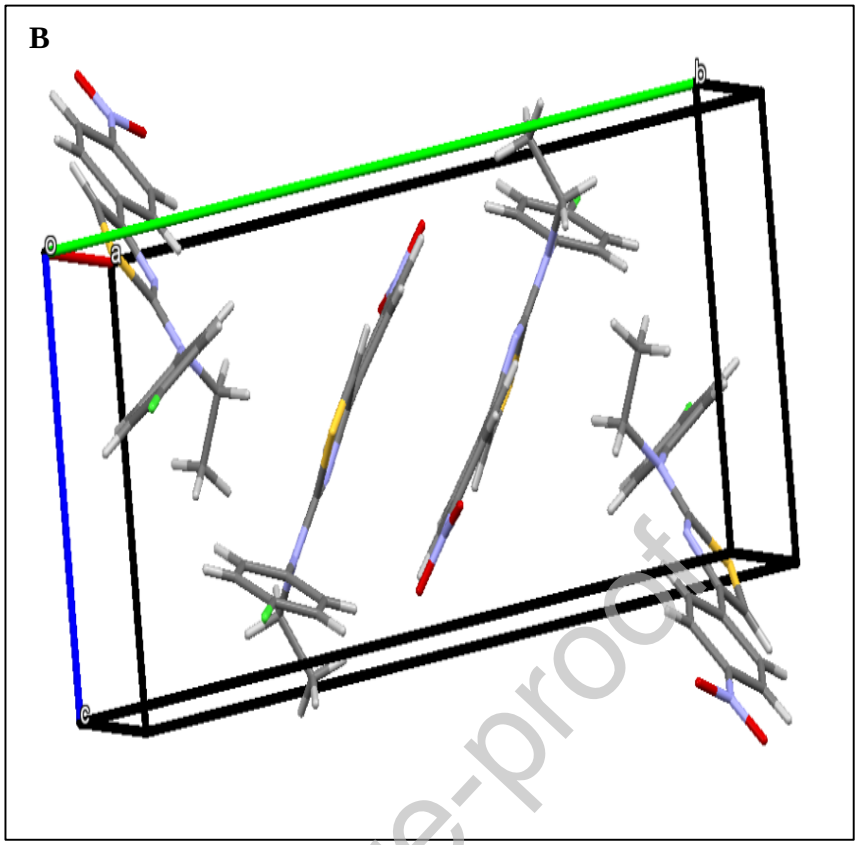

Fig.3. (B) Molecular packing of **3b**

Table 2. Selected bond lengths of **3a** and **3b**

Bond lengths (Å)	**3a**	**3b**
Cl1-C1	1.739(4)	1.738(2)
S1-C10	1.724(4)	1.714(18)
S1-C9	1.750(4)	1.746(16)
N2-C9	1.293(4)	1.298(2)
N2-C11	1.390(4)	1.386(18)
N1-C9	1.358(4)	1.353(19)
N1-C4	1.425(5)	1.430(2)
N1-C7	1.475(5)	1.465(2)
C15-C16	1.362(5)	1.374(2)
C15-C14	1.370(5)	1.381(2)
C14-C13	1.372(5)	1.374(2)
C13-C12	1.389(5)	1.394(2)
C12-C17	1.385(4)	1.396(2)
C12-C11	1.470(4)	1.465(2)
C11-C10	1.337(5)	1.351(2)
C4-C5	1.359(5)	1.381(2)
C4-C3	1.373(5)	1.373(3)

C5-C6	1.372(5)	1.378(3)
C6-C1	1.362(5)	1.369(3)
C1-C2	1.340(6)	1.369(3)
C2-C3	1.366(6)	1.376(3)
C7-C8	1.490(7)	1.480(3)
C17-C16	1.375(5)	1.370(2)
Br1-C15	1.893(3)	---
C8-C18	1.463(8)	
C15-N3	---	1.457(2)
O1-N3	---	1.222(19)
O2-N3	---	1.229(2)

Table 3. Selected bond angles of **3a** and **3b**

Bond angles (°)	**3a**	**3b**
C10-S1-C9	88.02(17)	88.20(8)
C9-N2-C11	110.4(3)	110.1(13)
C9-N1-C4	121.5(3)	119.1(14)
C9-N1-C7	119.7(3)	121.1(14)
C4-N1-C7	118.7(3)	119.6(13)
C16-C15-C14	120.6(3)	121.7(15)
C15-C14-C13	119.3(3)	118.7(16)
C14-C13-C12	121.6(3)	121.2(14)
C17-C12-C13	117.5(3)	118.0(15)
C17-C12-C11	121.7(3)	121.5(15)
C13-C12-C11	120.8(3)	120.4(13)
C10-C11-N2	115.3(3)	115.2(15)
C10-C11-C12	126.6(3)	126.2(14)
N2-C11-C12	118.1(3)	118.5(14)
N2-C9-N1	123.8(3)	124.9(14)
N2-C9-S1	115.0(2)	115.2(11)
N1-C9-S1	121.1(3)	119.7(13)
C5-C4-C3	118.9(4)	119.2(17)
C5-C4-N1	121.2(4)	120.4(15)
C3-C4-N1	119.8(4)	120.3(16)
C4-C5-C6	121.2(4)	120.5(17)
C1-C6-C5	118.3(4)	119.0(18)
C2-C1-C6	121.6(4)	121.3(19)
C2-C1-Cl1	118.9(3)	119.4(16)
C6-C1-Cl1	119.5(3)	119.2(16)
C1-C2-C3	119.8(4)	119.1(19)
C2-C3-C4	120.1(4)	120.6(19)

N1-C7-C8	109.6(4)	113.2(15)
C11-C10-S1	111.2(3)	111.1(12)
C16-C17-C12	121.0(3)	121.4(15)
C15-C16-C17	120.0(3)	118.8(14)
C18-C8-C7	114.0(6)	---
C16-C15-Br1	119.9(3)	---
C14-C15-Br1	119.5(3)	---
C16-C15-N3	---	119.0(13)
C14-C15-N3	---	119.2(15)
O1-N3-O2	---	122.5(15)
O1-N3-C15	---	118.7(15)
O2-N3-C15	---	118.7(14)

Table 4. Hydrogen bonding interactions (Å, °) for **3a** and **3b**.

D-H···A[a] interactions	d(D-H)/Å	d(H···A)/Å	d(D···A)/Å	D-H···A/°
3a				
C16 - H16···Cl1	0.930	2.865	3.742	157.6
C8 -H8···C16	0.930	2.877	3.771	161.7
3b				
N3 -O2···S1	1.229	3.045	4.078	141.3

The thiazole ring forms an angle of 71.19° with phenyl ring-A (C1–C6) and 31.94° with another phenyl ring-B (C12-C17) in compound **3a**. Whereas in compound **3b**, thiazole ring forms an angle of 80.79° with phenyl ring-A and 11.68° with another phenyl ring-B [**Fig.4. (A) and (B)].** The torsion angle of −4.27° and −3.13° exhibited by S1–C9–N1–C4 for **3a** and **3b** respectively, indicate that S1 and C4 are *cis* to each other, while the torsion angle of 178.0° and 173.6° exhibited by N2–C9–N1–C4 for **3a** and **3b** respectively, indicate that N2 and C4 are *trans* to each other.

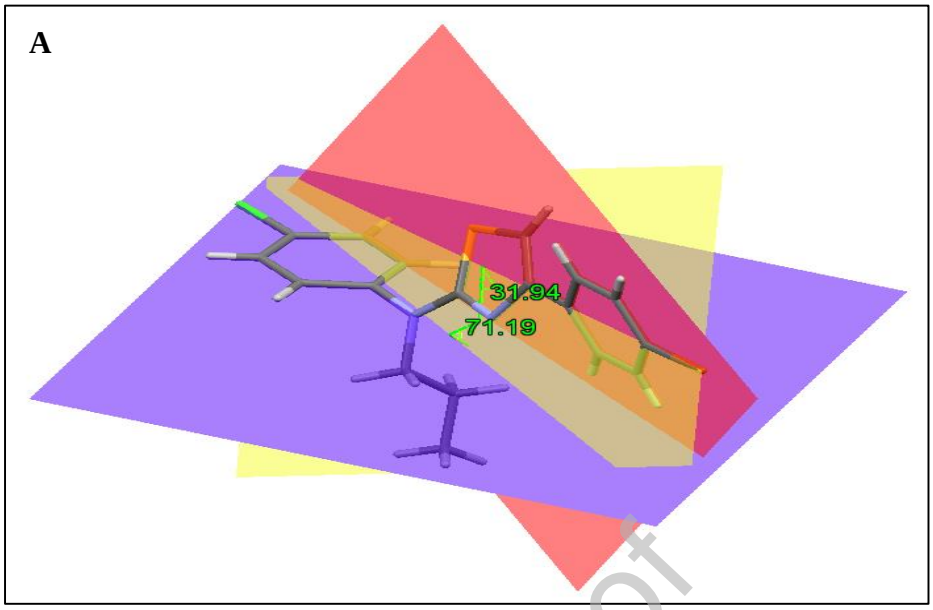

Fig.4. (**A**) Molecular planes of **3a**

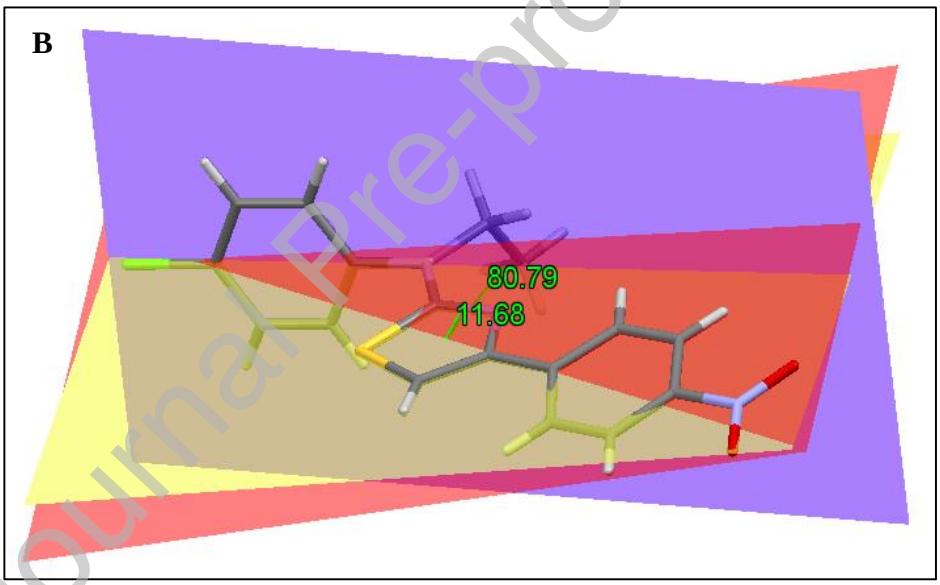

Fig.4. (**B**) Molecular planes of **3b**

Intermolecular Interaction

Crystal structure analysis revealed that the compounds exhibit different types of interactions and is the reason for their stability. The molecule **3a** is stabilized by strong intermolecular interactions like C1-Cl1···Cl1 (3.199 Å) and C10-H10···Cl1 (2.865 Å) and by C−H···π interaction between C5-H5 and thiazole (S1-C9-N1-C11-C10) ring (2.784 Å). Each individual molecule of **3a** is interconnected by weak π···π stacking interactions with a centroid–centroid distance of 5.676 Å connected between thiazole and phenyl rings of adjacent molecules. In case of **3b** it is stabilized by strong intermolecular interactions like C5-H5···O1 (2.691 Å), S1···O2

(3.045 Å) and by C−H···π interaction between C7-H7B and thiazole (S1-C9-N1-C11-C10) ring (2.899 Å) Stacking π···π interactions established between phenyl (C12-C17) rings of adjacent molecules of **3b** with centroid to centroid distances of 3.791 Å also stabilizes the structure. **(Fig.5 and 6**).

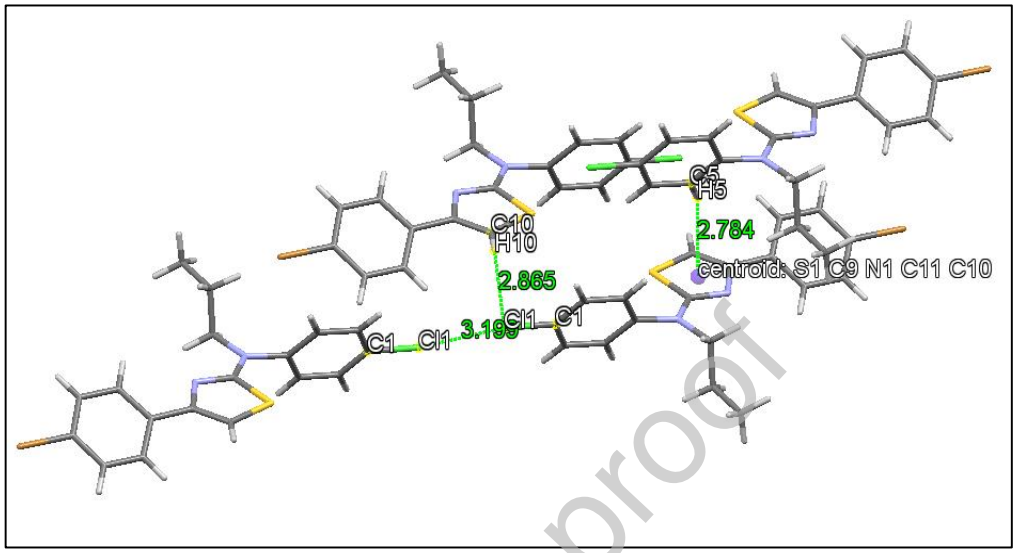

Fig.5. Intermolecular interactions shown by **3a**

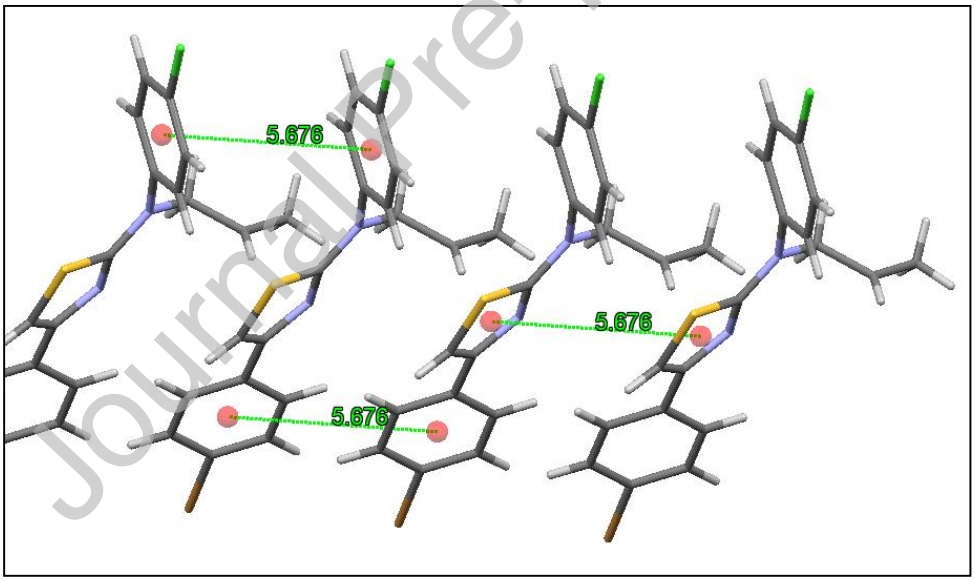

Fig.5b. Intermolecular π ···π interactions shown by **3a**

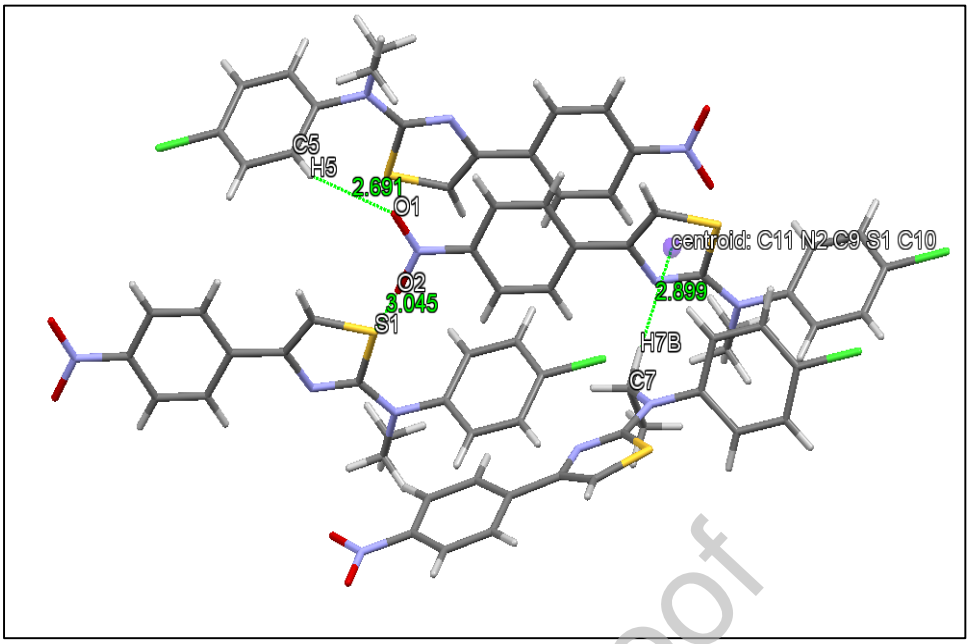

Fig.6. Intermolecular interactions shown by **3b**

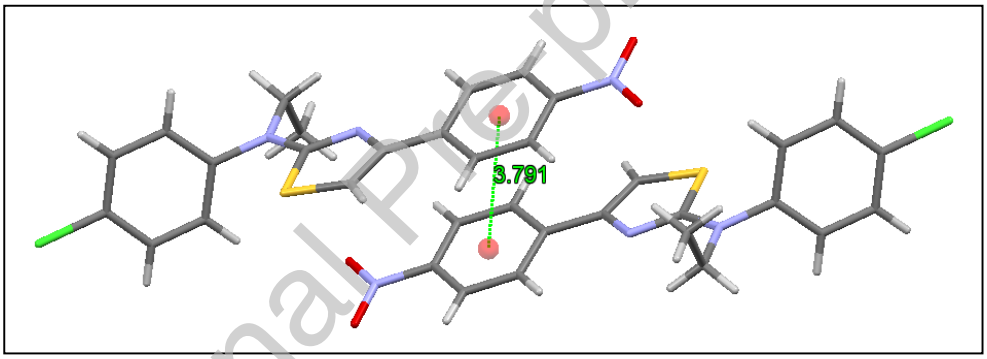

Fig.6b. Intermolecular π ···π interactions shown by **3b**

Hirshfeld surface analysis

Hirshfeld surface analysis is rapidly gaining importance as a useful technique in understanding the nature of intermolecular interactions within a crystal structure using a fingerprint plot. This allows easy identification of characteristic interactions throughout the structure. In order to measure various intermolecular interactions, HSs and their associated FPs were generated using Crystal Explorer 3.1. Even weak interactions, such as C−H···π, C···H and H···H contacts, which are hard to identify and are requisite for crystal packing, can be distinctly observed [41]. The Hirshfeld surface is defined by $w(r) = 0.5$, where the weight function $w(r)$ is given by the following equation,

$$w(r) = \frac{\sum_{i\varepsilon molecule}\rho i(r)}{\sum_{i\varepsilon crystal}\rho i(r)}$$

The weight function represents the ratio of the sum of spherical atom electron densities for a molecule to a similar sum for the entire crystal [36]. Several properties of HS can be envisioned and cyphered, in particular, d_e and d_i, which represent the distance from a point on the HS to the nearest nucleus outside or inside, respectively. The d_{norm} is the normalized contact distance and is defined by taking into account d_e and d_i and the van der Waals radii of the atoms as below:

$$d_{norm} = \frac{di\, r_i^{vdW}}{r_i^{vdW}} + \frac{de - r_e^{vdW}}{r_i^{vdW}}$$

Mapping d_{norm} on the HS gives a clear-cut and detailed picture of the interactions happening between adjacent molecules that are shorter than the van der Waals radii sum (visualized as red spots on the HS).

Hirshfeld surface analysis is a technique which reproduces the results of X-ray crystal structure analysis and helps to elucidate all the intermolecular interactions in a novel visual manner. This method uses visual recognition of properties of atom contacts through mapping of d_{norm} onto this surface. The increasing popularity of HS analysis comes from the fact that it allows recognition of less directional contacts, for instance, H/H dispersion forces. Another essential advantage is that all (d_i, d_e) contacts created by a molecule of interest can be expressed in the form of a two-dimensional (2D) plot, known as the 2D fingerprint plot. The d_e and d_i are defined, respectively, as the distance from the Hirshfeld surface to the nearest atom in the molecule itself and the distance from the surface to the nearest nucleus outwards from the surface. The shape of this plot, which is unique for each molecule, is determined by dominating intermolecular contacts [42]. The Hirshfeld surface mapped with a d_{norm} function (**Fig 7 and 8**) clearly shows dark red spot derived from C-H···Cl interactions in **3a** and form C-H···O interactions in **3b**, while the other intermolecular interactions appear as light-red spots. Red areas highlight intermolecular contacts shorter than the sum of the van der Waals radii. The 2D fingerprint plots are used to plot intercontacts with respect to d_i and d_e which shows that the most significant H···H interactions in both the compounds with contribution of 33.5 and 31.1 % in **3a** and **3b** respectively, next comes the C···H/H···C interactions characterized by wing like peripheral spikes (26.5 and 19.8 % in **3a** and **3b**, respectively).The non-directional H···H contacts are characterized by broader spikes is also a measure of strength of the crystal lattice. The other intercontacts of compound **3a** were found to be H···Cl/ Cl···H (10.9%), H···Br/ Br···H (14.3%), H···S/ H···S (7.7%), H···N/ H···N (2.3%). The major contributions are from H···H, H···C, H···Cl and H···Br when compared to

other intercontacts. The other intercontacts of compound **3b** were found to be H···Cl/ Cl···H (13.3%), H···O/ O···H (16.4%), H···S/ H···S (4.0%), H···N/ H···N (3.0%). The major contributions are from H···H, H···C, H···Cl and H···O when compared to other intercontacts (**Fig 9**).

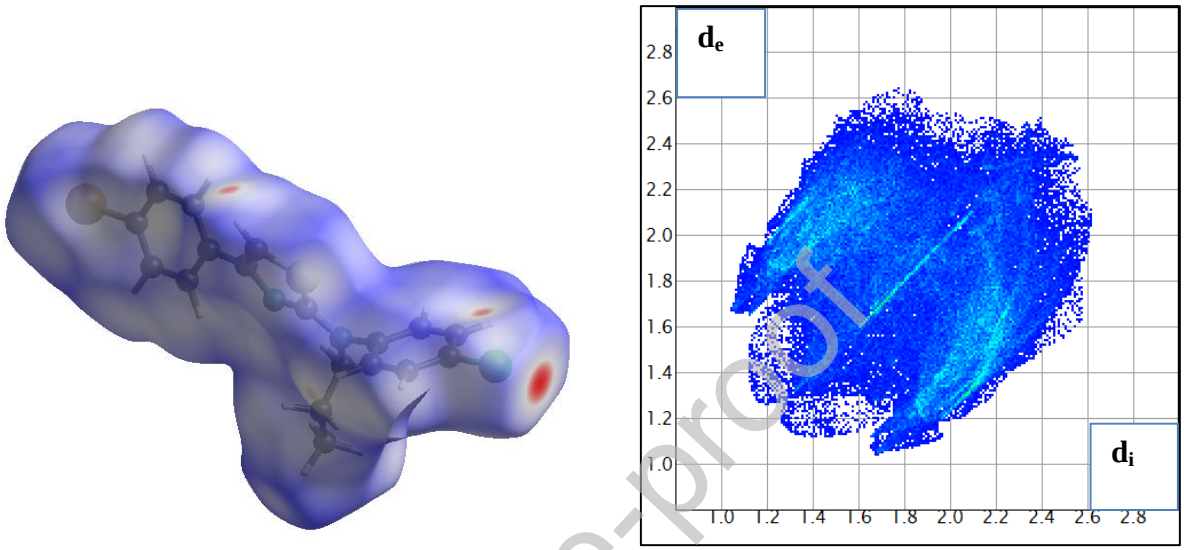

Fig.7. Hirshfeld surfaces mapped with *dnorm* and 2D fingerprint plot of **3a** depicting all intermolecular contributions.

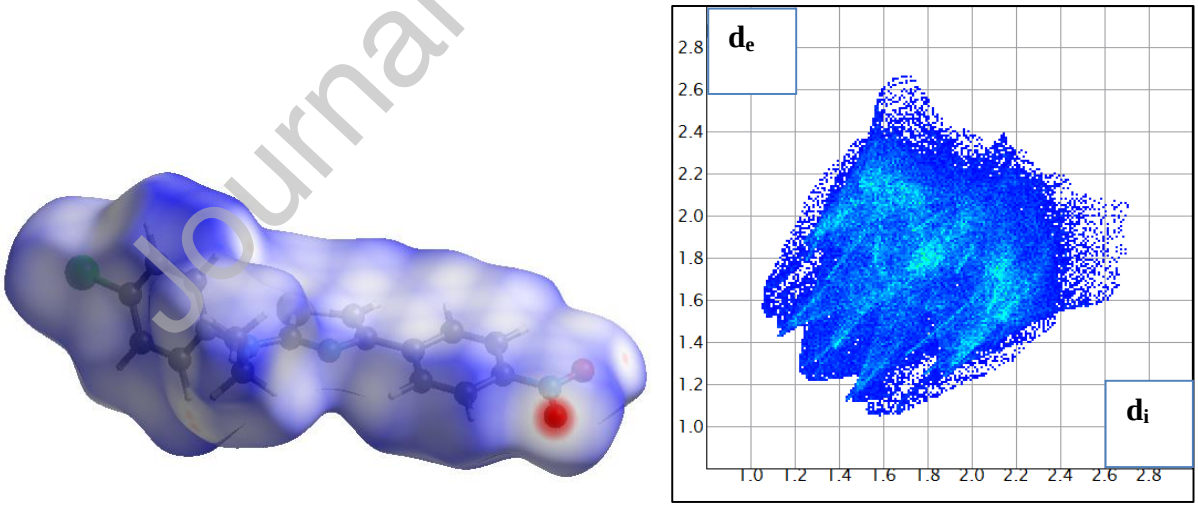

Fig.8. Hirshfeld surfaces mapped with *dnorm* and 2D fingerprint plot of **3b** depicting all intermolecular contributions.

---	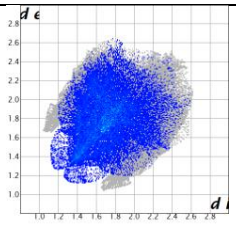	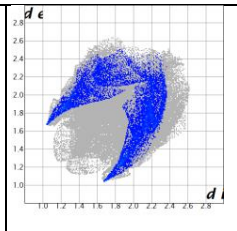	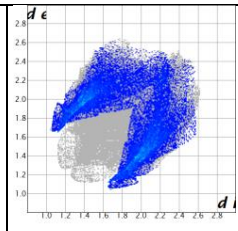	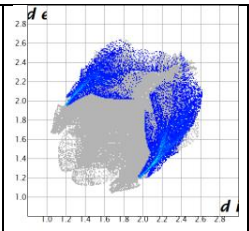	**3a**
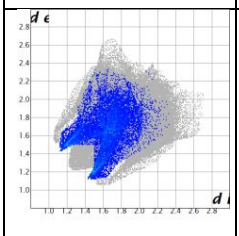	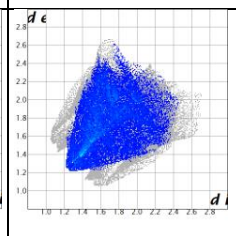	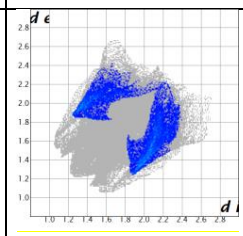	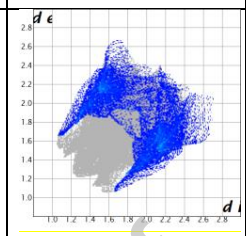	---	**3b**
O···H / H···O	H···H	Cl···H / H···Cl	C···H / H···C	H···Br/ Br···H	

Fig.9. 2D fingerprint plots of the **3a** and **3b** where areas of different intermolecular contacts are clearly shown; d_e and d_i are the distances to the nearest atom exterior and interior to the surface.

Conclusion

In the present work, 4-(4-bromophenyl)-*N*-(4-chlorophenyl)-*N*-propylthiazol-2-amine **(3a)** and *N*-(4-chlorophenyl)-*N*-ethyl-4-(4-nitrophenyl)thiazol-2-amine **(3b)** have been synthesized using an efficient and simple protocol. The synthesized compounds were characterized by analytical techniques like ^{1}H NMR, ^{13}C NMR, FT-IR and GCMS. Single crystal X-ray diffraction study revealed that they crystallized in triclinic, monoclinic system with P-1 and *P21/c* space group respectively. The asymmetric unit consists of only one molecule in both the structures. The crystal structures are stabilized by various C-H···π and π···π stacking interactions. The molecular Hirshfeld analysis and 2D fingerprint plots revealed the nature of molecular interactions and their contribution to the molecular surface. The intermolecular interactions are majorly H···H, O···H and C···H interactions which also aid in the stabilization of the molecules. This study supports to understand the molecular structures and the intermolecular interactions of substituted thiazole compounds.

Supplementary materials: CCDC **1945656** and CCDC **1945504** contain the supplementary crystallographic data which can be accessed from the Cambridge Crystallographic Data Centre:deposit@ccdc.cam.ac.uk.

Acknowledgements

The authors acknowledge University Scientific Instruments Centre (USIC and SAIF), Karnatak University, Dharwad for providing the spectral data and analytical facilities. DST-INSPIRE, New Delhi, India is greatly acknowledged for providing financial support under **DST/INSPIRE Fellowship/2016/IF160657** to the author **AfraQuasar A. Nadaf** and DST-PURSE PHASE-II program for providing necessary facilities. One of the authors Mahesh S. Najare is thankful to UGC-SRF for financial support.

Conflict of interest

Authors declare that there are no conflicts of interest.

References

1. V. S. Dinakaran, Der Pharm Chem. 4(1) (2012) 255-65.
2. M. Haroon, M. Khalid, T. Akhtar, M. N. Tahir, M. U. Khan, M. Saleem, R. Jawaria, J. Mol. Struct.1187 (2019) 164-171.
3. R. Mishra, P. K. Sharma, I. Tomer, G. Mathur, P. K. Dhakad, J. Heterocycl.Chem. 54(4) (2017) 2103–2116.
4. P. Fei Xua, Z. Hui Zhanga, X. Ping Huia, Z. Yi Zhanga, R. Liang Zhengb, J. Chin.Chem. Soc. 51 (2004) 315.
5. C. Ibis, A. F. Tuyun, Z. O. Gunes, H. Bahar, M.V. Stasevych, R.Y. Musyanovych, O. K. Porokhnyavets, V. Novikov, Eur. J. Med. Chem. 46 (2011) 5861.
6. A. K. Jain, A. Vaidya, V. Ravichandran, S. K. Kashaw, R. K. Agrawal, Bioorg. Med. Chem. 20 (2012) 3378.
7. J. F. Hartwig, Nature, 455(7211) (2008) 314.
8. N. Siddiqui, M. F. Arshad, W. Ahsan, M. S. Alam, Int. J. Pharm. Sci. Drug Res. 1 (2009) 136–143.
9. a) A. W. Hofmann, Ber. 12 (1879) 1126. b) A. W. Hofmann, Ber. 13 (1880) 8.
10. N. Siddiqui, M. F. Arshad, W. Ahsan, M. S. Alam, Int. J. Pharm. Sci. Drug Res. 1 (2009) 136.
11. A. Dondoni, A. Marra, Chem. Rev. 104 (2004) 2557.
12. N. A. A. Elkanzi, J. Chin. Chem. Soc. 65 (2018) 189.

13. Liebscher, J. Huben-Weyl's, Methoden der Organischen Chemie, E8b, 2 (1994) 1-399.
14. A. Saeed, P. A. Channar, G. Shabir, F. A. Larik, J. Fluoresc. 26 (2006) 1067.
15. L. M. Frija, A. J. Pombeiro, M. N. Kopylovich, Coord. Chem. Rev. 308 (2016) 32-55.
16. R. Hili, A. K. Yudin, Nat. Chem. Biol. 2(6) (2006) 284.
17. a) G. W. A. Milne, in: Ashgate (Ed.), Handbook of Antineoplastic Agents, Gower, London, UK, 2000.
    b) G.W. A. Das, P. Chen, D. Norris, R. Padmanabha, J. Lin, R. V. Moquin, Z. Shen, L. S. Cook, A. M. Doweyko, S. Pitt, S. Pang, D. R. Shen, Q. Fang, H. F. de. Fex, K. W. McIntyre, D. J. Shuster, K. M. Gillooly, K. Behnia, G. L. Schieven, J. Wityak, J. C. Barrish, J. Med. Chem. 49 (2006) 6819–32.
18. M.V.N. De Souza, M.V. De Almeida, Quim. Nova. 26 (2003) 366–372.
19. J. Das, P. Chen, D. Norris, R. Padmanabha, J. Lin, R. V. Moquin, Z. Shen, L. S. Cook, A. M. Doweyko, S. Pitt, S. Pang, J. Med. Chem. 49 (2006) 6819.
20. A. C. Pasqualotto, K. O. Thiele, L. Z. Goldani, Curr. Opin. Investig. Drugs 11 (2010) 165-74.
21. M. V. N. D. Souza, M. V. D. Almeida, Química Nova 26 (2003) 366.
22. L. M. Fox, L. D. Saravolatz, Clin. Infect. Dis. 40 (2005) 1173–1180.
23. D. Lednicer, L. A. Mitscher, G. I. George, in: Organic Chemistry of Drug Synthesis, 4 (1990) 95-97. 23. M. Z. Rehman, C. J. Anwar, S. Ahmad, Bull. Korean Chem. Soc. 26 (2005) 1771–1775.
24. M. P. Knadler, R. F. Bergstrom, J. T. Callaghan, A. Rubin, Drug Metab. Dispos. 14 (1986) 175–182.
25. R. Nauen, U. Ebbinghaus-Kintscher, V. L. Salgado, V. Kaussmann, Pest. Biochem. Physiol. 76 (2003) 55–69.
26. A. Hantzsch, J. H. Weber, Chem. Ber. 20 (1887) 3118.
27. (a) K. Dolling, H. Zaschke, H. Schubert, J. Prakt. Chem. 321 (1979) 643
    (b) A. A. Kiryanov, P. Sampson, A. J. Seed, J. Org. Chem. 66 (2001) 7925
    (c) A. Mori, A. Sekiguchi, K. Masui, T. Shimada, M. Horie, K. Osakada, M. Kawamoto, T. Ikeda, J. Am. Chem. Soc. 125 (2003) 1700.
28. Y. Wu, Y. Xie, Q. Zhang, H. Tian, W. Zhu, A.D.Q. Li, Angew. Chem. Int. Ed. 53 (2014) 2090.
29. B.Y. Kim, H. S. Kim, A. Helal, Sens. Actuators B-Chem. 206 (2015) 430.
30. T. Bach, S. Heuser, Tetrahedron Lett. 41 (2000) 1707.

31. K. Jana, T. Maity, S. Chandra Debnath, B. C. Samanta, S. K. Seth, J. Mol. Struct. 1130 (2017) 844-854.
32. C. A. Irena, K. Merijeta, M. Marko, B. Branimir, T. Sanja, P. Gordan, P. Kresimir, K. Z. Grace, Anal. J. Med. Chem. 52 (2009) 1744.
33. R. I. Cooper, A. L. Thompson, D. J. Watkin, J. Appl. Cryst. 43 (2010) 1100-1107.
34. P. W. Betteridge, J. R. Carruthers, R. I. Cooper, K. Prout, D. J. Watkin, J. Appl. Cryst. 36 (2003) 1487-1487.
35. D. J. Watkin, C. K. Prout, L. J. Pearce, CAMERON, Chemical Crystallography Laboratory, Oxford, England, 1996.
36. M. N. Burnett, C. K. Johnson, ORTEP-III: Oak Ridge Thermal Ellipsoid Plot Program for Crystal Structure Illustrations, Oak Ridge National Laboratory Report ORNL-6895, 1996.
37. G. M. Sheldrick, SHELXTL. Version 5.0, Bruker AXS Inc., Madison, Wisconsin, USA, 2001.
38. S. K. Wolff, D. J. Grimwood, J. J. McKinnon, M. J. Turner, D. Jayatilaka, M. A. Spackman, Crystal Explorer 3.1, University of Western Australia, Crawley, Western Australia, 2013, pp. 2005-2013.
39. M. A. Spackman, D. Jayatilaka, Cryst. Eng. Comm. 11 (2009) 19-32.
40. H. F. Clausen, M. S. Chevallier, M. A. Spackman, B. B. Iversen, New J. Chem. 34 (2010) 193.
41. M. A. Spackman, D. Jayatilaka, Cryst. Eng. Comm. 11 (2009) 19.
42. J. J. MacKimon, D. Jayatilaka, A. M. Spackman, Chem. Commun. 37 (2007) 3814-3816.